Collaborative target-tracking control using multiple autonomous fixed-wing UAVs with constant speeds

Collaborative target-tracking control using multiple autonomous fixed-wing UAVs with constant speeds: Theory and experiments

Zhiyong Sun, Héctor Garcia de Marina, Georg S. Seyboth, Brian D. O. Anderson, and Changbin Yu

Abstract—This paper considers a collaborative tracking control problem using a group of fixed-wing unmanned aerial vehicles (UAVs) with constant and non-identical speeds. The dynamics of fixed-wing UAVs are modelled by unicycle-type equations, with nonholonomic constraints by assuming that UAVs fly at constant altitudes in the nominal operation mode. The control focus is on the design of a collective tracking controller such that all fixed-wing UAVs as a group can collaboratively track a desired target's position and velocity. We first present conditions on the relative speeds of tracking UAVs and the target to ensure that the tracking objective can be achieved when UAVs are subject to constant speed constraints. We construct a reference velocity that includes both the target's velocity and position as feedback, which is to be tracked by the group centroid. In this way, all vehicles' headings are controlled such that the group centroid follows a reference trajectory that successfully tracks the target's trajectory. We consider three cases of reference velocity tracking: the constant velocity case, the turning velocity case with constant speed, and the time-varying velocity case. An additive spacing controller is further devised to ensure that all vehicles stay close to the group centroid trajectory. Trade-offs in the controller design and performance limitations of the target tracking control due to the constant-speed constraint are also discussed in detail. Experimental results with three fixed-wing UAVs tracking a target rotorcraft are shown to validate the effectiveness and performance of the proposed tracking controllers.

Index Terms—Fixed-wing UAV, target tracking, collaborative coordination, constant speed.

I. INTRODUCTION

A. Background and motivation

Large-scale operations involving search and rescue, disaster response, environmental monitoring and sport coverage are envisioned to be more cost-effective by making full use of networked multi-vehicle systems. One of the most active and important challenges in multi-vehicle systems is the control and coordination of a group of Unmanned Aerial Vehicles (UAVs) [1], [2], in particular, fixed-wing aircraft. A particular constraint complicating cooperative control design arises from constraints on their airspeeds. In practice, airspeeds for fixed-wing UAVs should lie in a bounded value interval: a lower bound for the UAV speed that guarantees they will not stall, and an upper bound arising from actuator constraints. In fact, small-sized fixed-wing aircraft typically fly optimally at *constant* airspeeds, which are usually designated nominal values designed for an optimal operation mode. For example, a constant speed might be given due to the optimization of the lift/drag ratio and as a consequence of having the vehicle's motor working in a nominal state with a fixed-pitch propeller. Furthermore, there often exists an optimal airspeed which is the most aerodynamically efficient speed for a given airframe of a fixed-wing UAV [3]. Such a speed constraint imposes additional challenges for coordination control of multiple fixed-wing UAVs.

Tracking control of stationary or moving targets by multiple fixed-wing UAVs has been a benchmark control problem in the field of multi-vehicle coordination control, which has found numerous applications in practice including target localization, surveillance and target orbiting [4]–[8]. The footprints in Fig. 1 show four aircraft and helicopters tracking cyclists in the Tour de France 2018. In many stages the cyclists were split in many different groups, making it almost impossible to track all of them at the same time with only four vehicles. The usage of coordinated UAVs might solve this problem where efficient aircraft must fly at their nominal air-speeds to cover a cycling tour stage that might last several hours. Fig. 2 shows two other typical scenarios involving multi-UAVs and target tracking, performed by the US military in a Perdix UAV swarm demonstration[1]. The demonstration employed almost 50 UAVs

Z. Sun is with the Department of Automatic Control, Lund University, SE-221 00 Lund, Sweden. Emails: `sun.zhiyong.cn@gmail.com`, `zhiyong.sun@control.lth.se`.

H. Garcia de Marina is with Unmanned Aerial Systems centre, The Maersk Mc-Kinney Moller Institute, University of Southern Denmark, DK-5230 Odense M, Denmark. Email: `hgm@mmmi.sdu.dk`.

G. S. Seyboth was with Institute for Systems Theory and Automatic Control, University of Stuttgart, Pfaffenwaldring 9, 70550 Stuttgart, Germany. He is now with Robert Bosch Automotive Steering GmbH, 73527 Schwaebisch Gmuend, Germany. Email: `georg.seyboth@googlemail.com`.

B. D. O. Anderson is with the School of Automation, Hangzhou Dianzi University, Hangzhou 310018, China, also with the Research School of Electrical, Energy and Material Engineering, Australian National University, Canberra, ACT 2601, Australia, and also with Data61-CSIRO, Canberra, ACT 2601, Australia. Email: `brian.anderson@anu.edu.au`.

C. Yu is with the Optus-Curtin Centre of Excellence in Artificial Intelligence, Curtin University, Perth, WA, Australia. Email: `brad.yu@curtin.edu.au`.

[1]Images in Fig. 2 are captured from the video released in https://www.dvidshub.net/video/504622/perdix-swarm-demo-oct-2016. Also see the news report http://www.bbc.com/news/technology-38569027, dated on 10 January 2017.
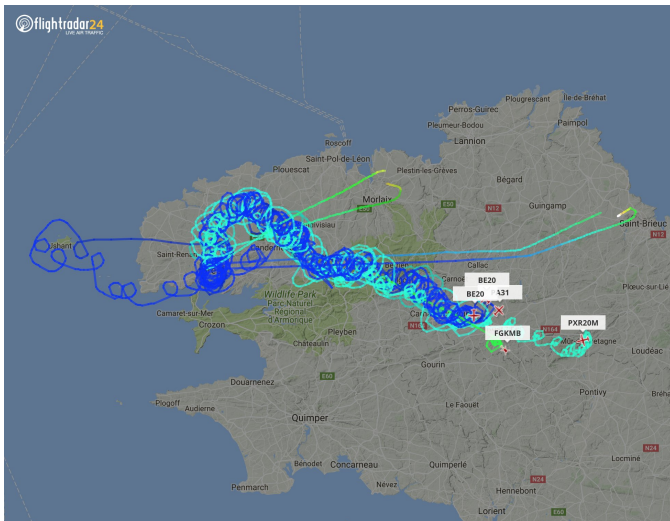
Fig. 1: Footprints of the aircraft and helicopters tracking and covering the 6th stage of Tour de France 2018. Courtesy of www.flightradar24.com.
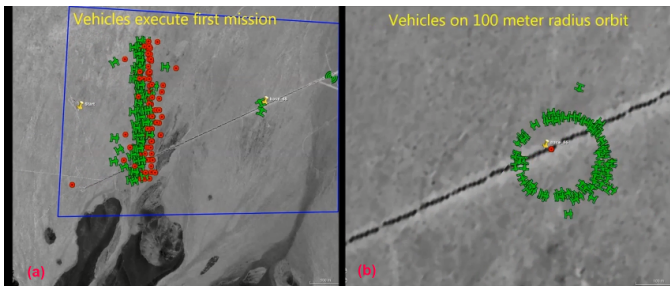

Fig. 2: Typical tracking task involving multiple UAVs in a swarm. (a) Target tracking; (b) target orbiting. The images are taken from the perdix micro-UAV swarm demonstration, released by the US Office of the Secretary of Defense Public Affairs in a public website www.dvidshub.net.

with adjustable cruising speeds and heading velocity, in a seemingly centralized control framework.

These examples motivate us to study and explore new approaches for the coordination control of a team of fixed-wing aircraft to perform a collaborative target-tracking task. By assuming that each vehicle flies at a constant altitude in a nominal operation mode, the dynamics of fixed-wing UAVs can be modelled by 2-D differential equations with nonholonomic motion constraints and constant speeds. This paper focuses on the design of feasible target-tracking controllers for multiple *autonomous* fixed-wing UAVs with motion and speed constraints to cooperatively track a moving target.

B. Related papers

The above-mentioned coordination problems become much more challenging if all UAVs in the group have speed constraints. In fact, a more realistic model than single- or double-integrators that can describe the nonholonomic constraints of such fixed-wing UAV dynamics is the unicycle model. Early contributions on coordination control of unicycle-type vehicles

include consensus-based formation control [9], pursuit formation design [10], and rendezvous control [11]. Other recent papers include different control constraints [5], [6], [12]–[16] to name just a few, but all assume that both the cruising speed and heading angular speed of individual vehicles are adjustable or controllable. For example, collaborative target-tracking guidance with fixed-wing UAVs was discussed in e.g., [4]–[6], [13] via several strategies such as *model predictive control* or *dynamic programing*. The tracking control of multiple unicycles was considered in [16], [17], in which a group of unicycles were tasked to track the trajectory of a target with a time-varying velocity and the framework of *circular motion* control proposed in [18] was employed. A more recent paper [19] relaxed measurement requirements on target information, but still assumed a unicycle-type model with control inputs relating to both cruising speed and angular speed. In this paper we will consider the more challenging tracking control problem when only the orientation can be controlled and the speeds of all the vehicles remain fixed, so as to reflect the consideration of speed constraints in certain types of real fixed-wing UAVs [2], [4], [8].

When a group of constant-speed vehicles are involved in the control task of trajectory tracking, the problem becomes even more challenging. Two fundamental tracking problems (on tracking a straight line trajectory or a circular trajectory without the consideration of velocity matching) were discussed in [18], [20]–[23], which assumed 2-D unicycle-type UAV models with *unit* speeds. In [18], [21] the authors showed how to control a group of *unit-speed* unicycles to achieve two behavior primitives (viz. circular motion and translational motion), with the switching between circling and aligned translation control. The papers [2], [24] investigated non-hierarchical formation control of a group of fixed-wing UAVs with speed constraints in performing surveillance tasks, while the control law is based on switching control that regulates the the centre of mass to follow a nominated (spiral) trajectory. The proposed technique in [22] showed a two-step design approach for designing tracking controllers that allows the formation centroid of a group of *unit-speed* unicycles to track a moving target. Such strategies were further explored in [25] for vision-based flocking control of multiple autonomous vehicles.

In this paper we further consider a more realistic scenario where constant speeds in a multi-UAV group are *not identical* (but may be similar in terms of their nominal values). This is motivated by practical tracking scenarios that a multi-vehicle group may consist of multiple *heterogeneous* UAVs with different functions or payloads, which will help to perform a comprehensive target-tracking task. Recent efforts towards the coordination of fixed-wing aircraft with *non-identical constant* speeds were presented in [26]–[28], which demonstrated coordination algorithms based on circular motions, rigid formations and distributed consensus-based flying coordination in practice. A general theory and experimental verification on target-tracking control with multiple fixed-wing UAVs with non-identical constant speeds are however lacking in the literature.

C. Contributions and paper organization

In this paper we aim to provide a systematic method to solve the target-tracking control problem under the constraints that (a) a target with a general trajectory curve is to be tracked, and (b) different vehicles have non-identical constant speeds. The framework for designing tracking controllers in this paper is motivated in part by [21], [22], but several significant extensions and novel designs are required to deal with heterogeneous vehicles with non-identical speeds to achieve a collaborative control task of tracking a general target trajectory. The controller design consists of two parts: reference velocity tracking that aims to regulate the group centroid to track a target's velocity and position, and a spacing control that ensures all vehicles stay close to the group centroid. This two-step controller design was suggested in [22] on unit-speed unicycle agents, while in this paper we further develop an implementable set of tracking controllers for fixed-wing UAVs (modelled by unicycle-type equations) with constant but non-identical speeds. Furthermore, a rigorous analysis on the stability of different equilibria and the convergence of velocity tracking dynamics is presented in detail. Due to the coordination constraints arising from constant speed, trade-offs in the controller design are inevitable and we also provide a detailed analysis on the performance limitations on using multiple fixed-wing UAVs in a collaborative tracking task.

A preliminary conference version of this paper was presented in [29]. The extensions of this paper compared to [29] include detailed proofs for all key results which were omitted in [29], the major additions that show convergence analysis of velocity tracking control with mobile targets, and discussions on the trade-offs and tracking limitations of using constant-speed UAVs in the target tracking task informed by experimental studies. Furthermore, a new section devoted to experimental verifications is also included in this extended version to demonstrate the real-life performance of the tracking controller. Thus, for the first time, this paper presents both theoretical solutions and experimental results on feasible tracking controllers for fixed-wing UAVs in autonomous target tracking tasks, and the findings will further advance real-life applications of fixed-wing UAVs, even under the strict conditions of constant cruising speed constraints.

We organize this paper as follows. We introduce the UAV model and problem formulation in Section II. Reference velocity tracking that ensures the UAV group centroid successfully tracks a reference trajectory is discussed in Section III, which also shows dedicated proofs on the convergence analysis of velocity tracking control with mobile targets. Section IV proposes the design of a reference velocity and spacing controller to ensure all vehicles move close to the group centroid. Experimental results with fixed-wing UAVs tracking a moving rotorcraft with the proposed collaborative tracking controller are shown in Section VI. Finally, Section VII concludes this paper.

II. BACKGROUND, PRELIMINARY AND PROBLEM DESCRIPTION

A. Notations

The notations used in this paper are fairly standard. The set $\mathbb{S}^1$ denotes the unit circle and an angle θ_i is a point $\theta_i \in \mathbb{S}^1$. The n-torus is the Cartesian product $\mathbb{T}^n = \mathbb{S}^1 \times \cdots \times \mathbb{S}^1$. For a complex number $z \in \mathbb{C}$, $\mathrm{Re}(z)$ and $\mathrm{Im}(z)$ denote, respectively, its real part and imaginary part, and $\bar{z}$ is the complex conjugate of z. For $z_1, z_2 \in \mathbb{C}^n$, the real scalar product is defined by $\langle z_1, z_2 \rangle = \mathrm{Re}(\bar{z}_1^T z_2)$, i.e., the real part of the standard scalar product over $\mathbb{C}^n$. The norm of $z \in \mathbb{C}^n$ is defined as $\|z\| = \langle z, z \rangle^{\frac{1}{2}}$. For two complex numbers $z_k = v_k e^{i\theta_k} \in \mathbb{C}$ and $z_j = v_j e^{i\theta_j} \in \mathbb{C}$ represented in the polar form, it holds

$$
\begin{aligned}
\langle z_k, z_j \rangle &= \mathrm{Re}(v_k e^{-i\theta_k} \cdot v_j e^{i\theta_j}) = \mathrm{Re}(v_k v_j e^{i(\theta_j - \theta_k)}) \\
&= \mathrm{Re}(v_k v_j \cos(\theta_j - \theta_k) + i v_k v_j \sin(\theta_j - \theta_k)) \\
&= v_k v_j \cos(\theta_j - \theta_k)
\end{aligned} \tag{1}
$$

and similarly,

$$
\begin{aligned}
\langle z_k, i z_j \rangle &= \mathrm{Re}(v_k e^{-i\theta_k} \cdot i v_j e^{i\theta_j}) = \mathrm{Re}(i v_k v_j e^{i(\theta_j - \theta_k)}) \\
&= \mathrm{Re}(i v_k v_j \cos(\theta_j - \theta_k) - v_k v_j \sin(\theta_j - \theta_k)) \\
&= v_k v_j \sin(\theta_k - \theta_j)
\end{aligned} \tag{2}
$$

Furthermore, the following equalities, whose simple proofs can be found in [27], will be used frequently later.

Lemma 1. *For $a, b \in \mathbb{C}^n$, there hold*

$$
\langle a, b\langle a, b \rangle \rangle = \langle b, a\langle a, b \rangle \rangle = \langle a, b\langle b, a \rangle \rangle = \langle a, b \rangle^2, \tag{3}
$$

and

$$
-\langle ia, b \rangle = \langle a, ib \rangle. \tag{4}
$$

B. Vehicle models

In this paper we consider a group of n fixed-wing vehicles modelled by unicycle-type kinematics subject to a nonholonomic constraint and constant-speed constraint. By following [4], [8], [13], the kinematic equations of fixed-wing vehicle k flying in a fixed horizontal plane are described by

$$
\begin{aligned}
\dot{x}_k &= v_k \cos(\theta_k) \\
\dot{y}_k &= v_k \sin(\theta_k) \\
\dot{\theta}_k &= u_k
\end{aligned} \tag{5}
$$

where $x_k \in \mathbb{R}, y_k \in \mathbb{R}$ are the coordinates of vehicle k in the real horizontal plane and θ_k is the heading angle. The fixed-wing UAVs have fixed cruising speeds $v_k > 0$ which in general are distinct for different vehicles; u_k is the control input to be designed for steering the orientation of vehicle k. The equation (5) serves as a high-level kinematic model, which captures well motion constraints and vehicle dynamics for fixed-wing UAVs flying at *trim* conditions (e.g., at constant altitudes or fixed level flight) [3]. In fact, the model (5) fits fairly well into the dynamics of a small fixed-wing aircraft as we have shown in [27], [28]. When an aircraft flies at its nominal airspeed, both its lift and weight are balanced so that there is no change in the vehicle's altitude. Therefore, the 3D dynamics of the aircraft can be easily decoupled to separate

the planar motion parallel to the ground, i.e., the dynamics (5), and the vertical motion. Consequently, we will assume that the aircraft fly at fixed (but different) altitudes in this paper, which is common in practical nominal operation of multi-UAV groups. Note that when the airspeed is much higher than the windspeed we can consider v_k as the ground speed [3]. As we will see during the experiments, this is a mild assumption that does not have a substantial impact on the performance of the proposed algorithm for the coordination of the aircraft.

For the convenience of analysis we also rewrite in complex notation the model (5) for vehicle k as

$$\dot{r}_k = v_k e^{i\theta_k} \tag{6a}$$

$$\dot{\theta}_k = u_k \tag{6b}$$

where the vector $r_k(t) = x_k(t) + iy_k(t) := \|r_k\|e^{i\phi_k(t)} \in \mathbb{C}$ denotes vehicle k's position in in the complex plane (where $\|r_k\| := \sqrt{x_k^2 + y_k^2}$ and $\phi_k := \arg(r_k)$). We also define the vectors $r = [r_1, r_2, \cdots, r_n]^T \in \mathbb{C}^n$, $\theta = [\theta_1, \theta_2, \cdots, \theta_n]^T \in \mathbb{T}^n$ and $e^{i\theta} = [e^{i\theta_1}, e^{i\theta_2}, \cdots, e^{i\theta_n}]^T \in \mathbb{C}^n$ to represent the stacked vectors of the positions, headings and rotations of all the vehicles, respectively.

C. Problem formulation

We consider the problem of tracking a target trajectory $r_{\text{target}}(t)$ by a team of fixed-wing UAVs with (possibly non-identical) constant speeds. A reasonable strategy in the multi-vehicle tracking control is to use the centroid of the vehicle team, denoted by $\hat{r}(t) = \frac{1}{n}\sum_{k=1}^{n} r_k(t)$, as the *surrogate* position of the whole vehicle group, which is to be controlled to match the target position $r_{\text{target}}(t)$. In fact, we will generate a velocity reference signal $\dot{r}_{\text{ref}}(t)$ to be tracked by the centroid in a manner previously introduced in [22]. As will be seen later in Section IV, this velocity reference signal is not necessarily identical to the target's velocity (unless initially the reference point is collocated with the target's position). The construction of the reference velocity takes into account both the target's velocity and the relative position between the target and the group centroid. The control strategy is split into two loops similarly to [30]. In a first phase discussed in Section III, an inner loop for each member of the UAV team controls their orientations so that the velocity of the centroid tracks $\dot{r}_{\text{ref}}(t)$. In a second phase discussed in Section IV, an outer loop generates $\dot{r}_{\text{ref}}(t)$ using information on the target's position.

We will see that our proposed controller for coordinating constant-speed UAVs resembles the phase control problem of coupled oscillators studied in [21], [26]. This is due to the fact that we will control angular velocities of the vehicles to regulate their heading orientations. An important measure for such an oscillator network is the so-called *order parameter* $p_\theta = \frac{1}{n}\sum_{k=1}^{n} e^{i\theta_k}$, which is actually the centroid velocity of a group of unit-speed vehicles and is often used to measure the phase coherence or phase synchronization level [18], [31]. In this paper we will use a similar metric called *average linear momentum* $\dot{\hat{r}} := \frac{1}{n}\sum_{k=1}^{n} v_k e^{i\theta_k}$ [26], which is actually the velocity of the group centroid point according to the definition of $\hat{r}$. The authors in [26] employ this metric for the control of circular motions of unicycles with different constant speeds, and one of our proposed controllers can be seen as an extension of that work.

Apart from the velocity reference tracking control by the group centroid, we also need to provide an extra control to steer each vehicle to stay close to the group centroid. For example, if we consider the position of the target is stationary at the origin, one may encounter situations where some or all of the tracking vehicles travel away from the origin while their centroid remains constant at the target, a situation which is not acceptable (except in the short term). We will therefore introduce an additional term to the tracking controller to regulate *the planar spacing* among the vehicles as a coherent tracking team. Consequently, all the vehicles will remain at a bounded distance from their centroid. In this work, we will not consider additional terms for collision avoidance. In particular, since one of our goals is to demonstrate the algorithm on fixed-wing aircraft, we can always suppose that they are flying at different altitudes. This should not be a strong restriction if we are not aiming at really massive swarms, and it is a common assumption in the literature [22], [26]. In summary, the overall tracking controller will be in the form

$$u_k = u_k^{\text{velocity}} + u_k^{\text{spacing}} \tag{7}$$

where u_k^{velocity} is the responsible term to track the reference velocity (which is constructed by feedback from a target's position and velocity) via the group centroid and the term u_k^{spacing} controls *the spacing* for each individual vehicle so that they can remain with a bounded distance to the centroid. The two-step controller design method (7) was also suggested in [22] for tracking control of unit-speed unicycles, while the development of tracking controllers for heterogeneous unicycle-type agents with constant but non-identical speeds requires substantial improvements and dedicated proofs on the stability and convergence property (which will be shown in Section III). Furthermore, it is obvious that there exist certain trade-offs in the design of these two controllers since, generally speaking, the two sub-tasks (i.e., reference velocity tracking and spacing control) are not likely to be achieved perfectly at the same time. Performance limitations arising from the trade-offs in the controller design will be discussed in more detail in Section III and Section IV.

III. CONTROLLER DESIGN PHASE I: REFERENCE VELOCITY TRACKING

In this section we discuss Phase I in the controller design, i.e., how to regulate each vehicle's heading and motion with the dynamics $\dot{\theta}_k = u_k^{\text{velocity}}$ so that the velocity of the vehicle group's centroid achieves a desired reference velocity. The construction of a reference velocity, the combined controller design that stabilizes the spatial error to the target's position and the spacings between individual vehicles will be discussed in the next section.

A. Conditions on constant speeds for a feasible reference velocity tracking

Denote the reference velocity by $\dot{r}_{\text{ref}}(t) = v_{\text{ref}}(t)e^{i\theta_{\text{ref}}(t)}$, where $v_{\text{ref}}(t)$ and $\theta_{\text{ref}}(t)$ are the (possibly time-varying) air-speed and heading direction of the reference, respectively.

If initially the reference trajectory coincides with the target trajectory, the target velocity is used as the reference velocity. Otherwise, the construction of the reference velocity should take into account both the target's position and velocity (which will be elaborated in detail in Section IV). For a group of constant-speed vehicles, one cannot expect that an arbitrary reference velocity can be tracked by the group centroid. In this section we will give several conditions that guarantee a feasible reference velocity tracking.

We recall the definitions of the group centroid position $\hat{r}$ and velocity $\dot{\hat{r}}$ as defined in Section II-C, whose values depend on the simultaneous headings and velocities of each individual vehicle. The maximum value of the group centroid speed, denoted as $\bar{v}_{\max}$, can be achieved when *all the vehicles reach a heading synchronization*, in which case there holds $\bar{v}_{\max} := \|\dot{\hat{r}}_{\max}\| = \frac{1}{n}\sum_{k=1}^{n} v_k$. However, due to the non-identical constant speeds in the group, even if the maximum group centroid speed $\bar{v}_{\max} = \frac{1}{n}\sum_{k=1}^{n} v_k$ can be achieved, the inter-vehicle distances between individual vehicle will grow larger and larger and eventually unboundedly because of the non-zero differences between individual speeds. Therefore, a strict condition on the individual speeds should be imposed.

For any vehicle in the group, the minimum speed, denoted by $v_{\min} := \min_{k \in \{1,2,\cdots,n\}} v_k$ should be greater than the reference speed $\|\dot{\hat{r}}_{\mathrm{ref}}(t)\|$. Otherwise, the distance between the vehicle with the smallest speed and the target will grow unboundedly and a collective target tracking can not be achieved. Therefore, one should ensure that the reference speed is smaller than the minimum speed in the vehicle group (which trivially ensures that the reference speed is smaller than any constant speed of the vehicle group). Of course, the reference speed cannot exceed the maximum speed of the group centroid $\frac{1}{n}\sum_{k=1}^{n} v_k$.

Now consider the case that the group centroid is able to achieve a zero centroid velocity, which is not possible if there exists one vehicle in the group whose constant speed is larger than the sum of all other vehicles' speeds. In order to ensure that the group centroid speed lies in the range $[0, v_{\min}]$, one should have $v_{\max} \leq \sum_{k=1}^{n} v_k - v_{\max}$. In summary, the necessary conditions for a feasible reference velocity tracking are shown in the following proposition.

Proposition 1. *For a feasible reference velocity tracking, the constant speeds for the vehicle group should satisfy the following conditions.*

- *All vehicles' speeds should be greater than the reference speed, i.e., $v_{min} \geq v_{ref}$;*
- *There does not exist one vehicle in the group whose speed is larger than the sum of the speeds of all other vehicles, i.e. there should hold $v_{max} \leq \sum_{k=1}^{n} v_k - v_{max}$.*

In the following subsections, we consider velocity tracking control for the constant-speed vehicle group. We will start from the simple case of constant reference velocity and then extend the controller design result to the time-varying velocity case.

B. Tracking a constant reference velocity

This subsection solves the control problem of regulating the formation centroid to track and match a constant reference velocity $\dot{r}_{\mathrm{ref}} = v_{\mathrm{ref}} e^{i\theta_{\mathrm{ref}}}$, in which both v_{ref} and θ_{ref} are constant. The controller involves collectively regulating the heading of each individual vehicle. This control problem can be seen as an extension of the result in [18], [20] which discussed the control problem of regulating a group of *unit-speed* vehicles to achieve a flocking behavior (i.e. a translational motion along a fixed direction).

The first main result on constant velocity tracking is stated in the following theorem.

Theorem 1. *Suppose that the constant reference velocity v_{ref} and all vehicles' constant speeds v_k satisfy the conditions in Proposition 1. Consider the following steering control law for (6)*

$$
\begin{aligned}
u_k^{velocity} &= -\gamma \left\langle \dot{\hat{r}} - \dot{r}_{ref}, \frac{1}{n} i v_k e^{i\theta_k} \right\rangle \\
&= -\gamma \left\langle \frac{1}{n}\sum_{k=1}^{n} v_k e^{i\theta_k} - v_{ref} e^{i\theta_{ref}}, \frac{1}{n} i v_k e^{i\theta_k} \right\rangle \quad (8)
\end{aligned}
$$

where γ is a positive control gain. Suppose that the initial headings of all the vehicles are not aligned with the phase of the reference velocity. Then the equilibrium point for the phase dynamics (6b) at which $\dot{\hat{r}} := \frac{1}{n}\sum_{k=1}^{n} v_k e^{i\theta_k} = v_{ref} e^{i\theta_{ref}}$ is asymptotically stable and all other equilibria are unstable. Furthermore, the control law (8) almost globally stabilizes the group centroid velocity to the desired constant reference velocity $\dot{r}_{ref} = v_{ref} e^{i\theta_{ref}}$.

We remark that the second term in (8), i.e., $i v_k e^{i\theta_k}$, essentially rotates the complex variable $v_k e^{i\theta_k}$ by 90 degrees. The control input can also be written using real variables with trigonometric functions, by using the formulas introduced in Section II-A.

Proof. We first show that the system $\dot{\theta} = u^{\mathrm{velocity}}$ with the above designed controller (8) describes a gradient flow for the following quadratic potential

$$
\begin{aligned}
V(\theta) &= \frac{1}{2}\|\dot{\hat{r}} - \dot{r}_{\mathrm{ref}}\|^2 \\
&= \frac{1}{2}\left\langle \frac{1}{n}\sum_{k=1}^{n} v_k e^{i\theta_k} - v_{\mathrm{ref}} e^{i\theta_{\mathrm{ref}}}, \frac{1}{n}\sum_{k=1}^{n} v_k e^{i\theta_k} - v_{\mathrm{ref}} e^{i\theta_{\mathrm{ref}}} \right\rangle
\end{aligned}
$$
$$(9)$$

The gradient of $V(\theta)$ can be calculated as

$$
\begin{aligned}
\frac{\partial V(\theta)}{\partial \theta_k} &= \left\langle \frac{\partial \dot{\hat{r}}}{\partial \theta_k}, \dot{\hat{r}} - \dot{r}_{\mathrm{ref}} \right\rangle \\
&= \left\langle \frac{1}{n} i v_k e^{i\theta_k}, \dot{\hat{r}} - \dot{r}_{\mathrm{ref}} \right\rangle = \left\langle \dot{\hat{r}} - \dot{r}_{\mathrm{ref}}, \frac{1}{n} i v_k e^{i\theta_k} \right\rangle
\end{aligned}
$$
$$(10)$$

Hence the phase system (6b) with the designed control law (8) can be written as $\dot{\theta} = -\gamma \nabla V(\theta)$ which is a gradient descent flow for the potential function $V(\theta)$. Furthermore, $V(\theta) \geq 0$ and $V(\theta)$ is zero if and only if $\dot{\hat{r}} = \dot{r}_{\mathrm{ref}}$. Thus, $V(\theta)$ can be
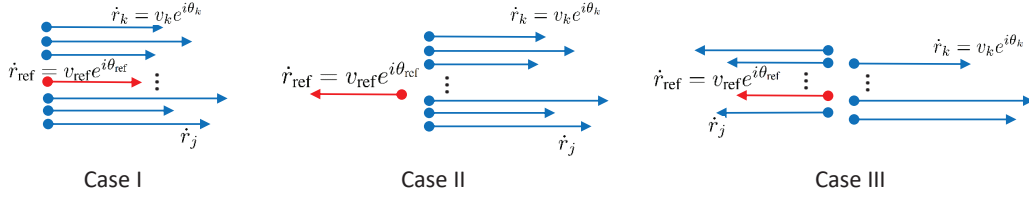
Fig. 3: Illustrations of three cases of undesired equilibria under which $\|\dot{\tilde{r}}\| > 0$ and $\sin(\phi - \theta_k) = 0, \forall k$. (a) Case I: $m = 0$; (b) Case II: $m = n$; (c) Case III: $1 \leq m \leq n - 1$.

used as a Lyapunov function for the convergence analysis. Due to the gradient property of the phase system (6b), there exists no limit cycle under the control $\dot{\theta} = u^{\text{velocity}}$ at the steady state [32]. Furthermore, the stability analysis of different equilibria (6) can be cast as a critical point analysis of the real analytic potential $V(\theta)$. Note that the system variable is $\theta \in \mathbb{T}^n$ where $\mathbb{T}^n$ is compact and thus the sub-level sets of $V(\theta)$ are also compact according to its definition in (9). We remark that for the phase dynamics (6b) with the velocity tracking controller (8), the state variable is θ while r is not involved. [2]

The derivative of $V(\theta)$ along the trajectory of the phase system (6) can be computed as

$$\dot{V} = \nabla V(\theta)^T \dot{\theta} = -\frac{\gamma}{n} \sum_{k=1}^{n} \left\langle \dot{\hat{r}} - \dot{r}_{\text{ref}}, iv_k e^{i\theta_k} \right\rangle^2 \leq 0 \quad (11)$$

By LaSalle's Invariance Principle, all solutions of (6) with the controller (8) converge to the largest invariant set contained in

$$\begin{aligned} \mathcal{O}(r, \theta) &= \{(r, \theta) | \dot{V} = 0\} \\ &= \{(r, \theta) | \left\langle \dot{\hat{r}} - \dot{r}_{\text{ref}}, iv_k e^{i\theta_k} \right\rangle = 0, \ k = 1, 2, \cdots, n\} \end{aligned}$$
$$(12)$$

In the following we will show the properties of different sets of critical points. Note that the Jacobian of the right-hand side of (6) with the controller (8) is $-\gamma H_V$ where H_V is the Hessian of V. The nature of an equilibrium (of being a minimum, a saddle point or a maximum) can be determined by the signs of the eigenvalues of the Hessian H_V at that equilibrium assuming that the Hessian is non-singular.

From the above analysis, it is clear that the desired critical points on which $\dot{\hat{r}} := \frac{1}{n} \sum_{k=1}^{n} v_k e^{i\theta_k} = v_{\text{ref}} e^{i\theta_{\text{ref}}} =: \dot{r}_{\text{ref}}$ are global minima of $V(\theta)$ which are asymptotically stable. We will show other equilibrium sets, which correspond to $V(\theta) > 0$, or equivalently equilibrium points in the set $\mathcal{O}(r, \theta)$ in (12) with $\left\langle \dot{\hat{r}} - \dot{r}_{\text{ref}}, iv_k e^{i\theta_k} \right\rangle = 0$ and $\dot{\hat{r}} \neq \dot{r}_{\text{ref}}$, are unstable. Denote the velocity tracking error as

$$\begin{aligned} \dot{\tilde{r}} &:= \dot{\hat{r}} - \dot{r}_{\text{ref}} = \frac{1}{n} \sum_{k=1}^{n} v_k e^{i\theta_k} - v_{\text{ref}} e^{i\theta_{\text{ref}}} \\ &= \|\dot{\tilde{r}}\| e^{i\phi} \end{aligned} \quad (13)$$

where $\|\dot{\tilde{r}}\|$ is the magnitude of $\dot{\tilde{r}}$, and $\phi := \arg(\dot{\tilde{r}})$ by definition. We call such critical points for which $\|\dot{\tilde{r}}\| > 0$ *undesired equilibria* since they do not achieve a desired reference velocity tracking.

Note that at an equilibrium point

$$\begin{aligned} \left\langle \dot{\hat{r}} - \dot{r}_{\text{ref}}, iv_k e^{i\theta_k} \right\rangle &= \left\langle \|\dot{\tilde{r}}\| e^{i\phi}, iv_k e^{i\theta_k} \right\rangle \\ &= \|\dot{\tilde{r}}\| v_k \sin(\phi - \theta_k) = 0 \end{aligned}$$

Therefore, at the undesired equilibria there holds $\sin(\phi - \theta_k) = 0$ for all $k = 1, 2, \cdots, n$, which implies that either $\theta_k = \phi \bmod 2\pi$ or $\theta_k = \phi + \pi \bmod 2\pi$. Let m be the number of vehicles with phase $(\phi + \pi \bmod 2\pi)$ at one of such undesired equilibria. The three cases of the undesired equilibria are illustrated in Fig. 3. Now consider two extreme cases:

- The case that $m = 0$ indicates that all the vehicles have the same phase $(\phi \bmod 2\pi)$. An undesired equilibrium with $m = 0$ is a local maximum of $V(\theta)$ and a small variation of any θ_k will decrease the value of $V(\theta)$. Therefore, any equilibrium with $m = 0$ and $\|\dot{\tilde{r}}\| > 0$ is unstable. [3]

- The case that $m = n$ indicates that all the vehicles have the same phase $(\phi \bmod \pi)$. According to (13) this implies that $\dot{\hat{r}} - \dot{r}_{\text{ref}} = \frac{1}{n} \sum_{k=1}^{n} v_k e^{i(\phi+\pi)} - v_{\text{ref}} e^{i\phi} = (\frac{1}{n} \sum_{k=1}^{n} v_k + v_{\text{ref}}) e^{i(\phi+\pi)}$ which is a global maximum of $V(\theta)$ where a small variation of any θ_k will decrease the value of $V(\theta)$. Therefore, any equilibrium with $m = n$ is unstable.

In the following, we will show that all other equilibria with $1 \leq m \leq n - 1$ are all saddle points. Without loss of generality, we renumber the vehicles such that the first m vehicles are with phase $(\phi + \pi \bmod 2\pi)$. The diagonal entries of the Hessian of V can be calculated as

$$\frac{\partial^2 V}{\partial \theta_k^2} = \begin{cases} (1/n)v_k^2 + \|\dot{\tilde{r}}\| v_k, & k \in \{1, \cdots, m\} \\ (1/n)v_k^2 - \|\dot{\tilde{r}}\| v_k, & k \in \{m+1, \cdots, n\} \end{cases}$$

and the off-diagonal entries are

$$\begin{aligned} \frac{\partial^2 V}{\partial \theta_j \partial \theta_k} &= (1/n)v_j v_k \cos(\theta_j - \theta_k) \\ &= \begin{cases} (1/n)v_j v_k, & j, k \in \{1, \cdots, m\} \\ & \text{or } j, k \in \{m+1, \cdots, n\} \\ -(1/n)v_j v_k, & \text{else} \end{cases} \end{aligned}$$

Therefore, the Hessian can be written in a compact form

$$H_V = \frac{1}{n} vv^T + \|\dot{\tilde{r}}\| \text{diag}(v) \quad (14)$$

---

[2] This point will be made clear in Remark 2, in which the control input is equivalently written in real variables that only involve θ.

[3] In the special case that all vehicles have the same constant speed v which is identical to v_{ref}, i.e., $v_k = v = v_{\text{ref}}, \forall k$, the case of $m = 0$ implies that $\dot{\tilde{r}} = 0$ which is a desired equilibrium and is stable.

where the vector v is defined as

$$v = [v_1, \cdots, v_m, -v_{m+1}, \cdots, -v_n]^T.$$

Since there exists at least one diagonal entry in the form of $(1/n)v_k^2 + \|\dot{\tilde{r}}\|v_k$ which is positive, the Hessian H_V has at least one positive eigenvalue. We will show the Hessian H_V has at least one negative eigenvalue at any critical point with $1 \leq m \leq n-1$ by proving that there exist vectors $q^- \in \mathbb{R}^n$ such that $q^{-T} H_V q^- < 0$. We first consider the case of $m = n-1$, which can happen if and only if the vehicle with maximum speed has phase (ϕ mod 2π) which is also the phase for the reference velocity. Define $q^- = [a_1, ..., a_{n-1}, 1]^T$, where the constant a_i satisfies $0 \leq a_i < 1$ for $i = 1, \cdots, n-1$ and $v^T q^- = 0$. Note that according to Proposition 1, such non-negative a_i always exists and cannot all be zero, which guarantees the existence of the vector q^-. Then a simple calculation yields $q^{-T} H_V q^- = \sum_{i=1}^{n-1} a_i^2 v_i - v_n = \sum_{i=1}^{n-1}(a_i^2 v_i - a_i v_i) < 0$. Therefore, an equilibrium point with $m = n-1$ is a saddle point and is therefore unstable.

We then consider the case of $1 \leq m < n-1$. Actually there are many options for constructing such a vector q^-. Without loss of generality, let us choose

$$q^- = [0, \cdots, 0, -v_n, v_{n-1}]^T \tag{15}$$

The existence of such q^- in (15) is guaranteed because $m < n-1$. Note that there holds $v^T q^- = 0$. It then follows that

$$\begin{aligned} q^{-T} H_V q^- &= \|\dot{\tilde{r}}\| q^{-T} \text{diag}(v) q^- \\ &= \|\dot{\tilde{r}}\|(-v_{n-1}^2 v_n - v_{n-1} v_n^2) < 0 \end{aligned} \tag{16}$$

Hence, it is proved that such critical points with $1 \leq m < n-1$ are saddle points and therefore are unstable. Consequently, all the undesired equilibria with $\langle \dot{\hat{r}} - \dot{r}_{\text{ref}}, iv_k e^{i\theta_k} \rangle = 0$ and $\dot{\hat{r}} \neq \dot{r}_{\text{ref}}$ are unstable.

In summary, the above arguments have proved that the desired equilibria at which $\dot{\hat{r}} = \dot{r}_{\text{ref}}$ are asymptotically stable, and all other equilibria are unstable. The initial points at which the initial headings of all the vehicles are aligned are excluded in the set of initial positions because these points correspond to unstable equilibria. $\square$

Remark 1. *The result on the reference velocity tracking in Theorem 1 is relevant and applicable to the target-tracking scenario in which initially the target position is the same as the centroid position, and the target velocity is constant (which, as will be discussed in Section IV, is used as the reference velocity). Extensions for time-varying velocity tracking will be discussed in the sequel. We also remark that since the group centroid is tasked to track a reference trajectory, an average of the positions and headings of all vehicles in the group should be calculated and therefore a complete graph is assumed in the reference velocity control to facilitate the calculation. This is justified by the all-to-all communication, a commonly-used assumption in the literature on fixed-wing UAV coordination control. Such an assumption may be relaxed by some consensus-based estimation technique (which only requires connectivity for an underlying communication graph)*

but will be traded-off by additional computation overhead for each vehicle, and therefore is not considered in this paper.

Remark 2. (*Control input in real variables*) *Theorem 1 can be seen as an extension of [26, Theorem 2], which considered the stabilization problem of the average linear momentum when $\dot{r}_{ref} = 0$. The above controller involves complex numbers and scalar products of complex vectors. For the implementation, one can calculate the control input (8) in real variables:*

$$\begin{aligned} u_k^{velocity} &= -\gamma \left\langle \dot{\hat{r}} - \dot{r}_{ref}, iv_k e^{i\theta_k} \right\rangle \\ &= -\frac{\gamma}{n} \left\langle \sum_{j=1}^n v_j e^{i\theta_j}, iv_k e^{i\theta_k} \right\rangle + \gamma \left\langle \dot{r}_{ref}, iv_k e^{i\theta_k} \right\rangle \\ &= -\frac{\gamma}{n} \sum_{j=1}^n v_k v_j \sin(\theta_j - \theta_k) + \gamma v_k v_{ref} \sin(\theta_{ref} - \theta_k) \end{aligned} \tag{17}$$

The phase dynamics (6b) with the controller (17) written using real variables has a similar form to the Kuramoto oscillator model which has been studied extensively [31], [33], but the difference is that the speed term is involved in (17) for controlling non-identical constant-speed vehicles. If we assume all vehicles have the same unit speed, the controller (17) then reduces to the one studied in [18], [20], [22] where the oscillator synchronization theory [31], [33] can apply.

C. Tracking a turning reference velocity with constant speed

In this subsection we consider the tracking control with a reference trajectory with constant speed and turning angular velocity. Motivated by [21] and [22], the target dynamics are described by

$$\begin{aligned} \dot{r}_{\text{ref}} &= v_{\text{ref}} e^{i\theta_{\text{ref}}} \\ \dot{\theta}_{\text{ref}} &= \kappa_{\text{ref}} \end{aligned} \tag{18}$$

where v_{ref} is the constant speed of the reference velocity and κ_{ref} is the angular velocity, which can be constant or non-constant and corresponds to the scaled curvature of the trajectory generated by the velocity. In the case of tracking a time-varying reference velocity with a constant speed, the essence of the velocity tracking control is to design a reference velocity matching controller such that the *constant reference speed* and the *trajectory curvature* can be tracked. The main result is summarized in the following theorem.

Theorem 2. *Suppose the turning reference velocity and all vehicles' constant airspeeds v_k satisfy the conditions in Proposition 1 and the initial headings of all the vehicles are not aligned with the initial phase of the reference velocity. Consider the following steering control law*

$$u_k^{velocity} = h_k - \gamma \left\langle \dot{\hat{r}} - \dot{r}_{ref}, iv_k e^{i\theta_k} \right\rangle \tag{19}$$

where $\hat{r}$ is the group centroid position, $\dot{\hat{r}}$ is the group centroid velocity as defined previously, γ is a positive control gain and the h_k are any real control terms that satisfy

$$\frac{1}{n} \sum_{k=1}^n iv_k e^{i\theta_k} h_k = iv_{ref} e^{i\theta_{ref}} \kappa_{ref} \tag{20}$$

Then the equilibrium point for the phase dynamics (6b) *at which $\dot{\hat{r}} = \dot{r}_{ref}$ is asymptotically stable and all other equilibria are unstable. The above control law will almost globally asymptotically stabilize the group centroid velocity of the multi-vehicle group* (6) *to the desired reference velocity $\dot{r}_{ref}$* (18).

Theorem 2 is a generalization of Theorem 1. If the time-varying component $\dot{\theta}_{ref} = \kappa_{ref}$ of the turning reference velocity is zero, then the control (19) can be reduced to the one in Theorem 1 as one can take all h_k equal to zero.

Proof. The proof can be seen as an extension of the proof for Theorem 1. Note that

$$\ddot{\hat{r}} = \frac{1}{n}\sum_{k=1}^{n} v_k e^{i\theta_k} i\dot{\theta}_k = \frac{1}{n}\sum_{k=1}^{n} iv_k e^{i\theta_k} u_k^{\text{velocity}} \quad (21)$$

and

$$\ddot{r}_{\text{ref}} = iv_{\text{ref}} e^{i\theta_{\text{ref}}} \kappa_{\text{ref}} \quad (22)$$

Then the dynamics for the velocity tracking error can be written as

$$\begin{aligned}
\ddot{\tilde{r}} &= \ddot{\hat{r}} - \ddot{r}_{\text{ref}} \\
&= \frac{1}{n}\sum_{k=1}^{n} iv_k e^{i\theta_k} u_k^{\text{velocity}} - iv_{\text{ref}} e^{i\theta_{\text{ref}}} \kappa_{\text{ref}} \\
&= -\frac{1}{n}\sum_{k=1}^{n} iv_k e^{i\theta_k} \gamma \left\langle \dot{\hat{r}} - \dot{r}_{\text{ref}}, iv_k e^{i\theta_k} \right\rangle
\end{aligned} \quad (23)$$

Consider the same Lyapunov-like function $V = \frac{1}{2}\|\dot{\hat{r}} - \dot{r}_{\text{ref}}\|^2$ as used earlier in studying the convergence analysis. Note that $V(\dot{\tilde{r}}) \geq 0$ and $V(\dot{\tilde{r}})$ is zero if and only if $\dot{\hat{r}} = \dot{r}_{\text{ref}}$, or equivalently $|\dot{\tilde{r}}| = 0$.

The derivative of V along the trajectories of the velocity tracking error system (23) can be calculated as

$$\begin{aligned}
\dot{V} &= \left\langle \dot{\hat{r}} - \dot{r}_{\text{ref}}, \ddot{\hat{r}} - \ddot{r}_{\text{ref}} \right\rangle \\
&= \left\langle \dot{\hat{r}} - \dot{r}_{\text{ref}}, -\frac{1}{n}\sum_{k=1}^{n} iv_k e^{i\theta_k} \gamma \left\langle \dot{\hat{r}} - \dot{r}_{\text{ref}}, iv_k e^{i\theta_k} \right\rangle \right\rangle \\
&= -\frac{\gamma}{n}\sum_{k=1}^{n} \left\langle \dot{\hat{r}} - \dot{r}_{\text{ref}}, iv_k e^{i\theta_k} \right\rangle^2 \leq 0
\end{aligned} \quad (24)$$

By LaSalle's Invariance Principle and similar arguments as in the proof of Theorem 1, it can be proven that the solution of (6) converges to a stable equilibrium in the largest invariant set in which $\dot{\tilde{r}} = 0$, which is equivalent to $\dot{\hat{r}} = \dot{r}_{\text{ref}}$ indicating that the time-varying reference velocity can be successfully tracked in the limit. □

Remark 3. *The conditions in Proposition 1 guarantee the existence of the desired equilibrium $\dot{\hat{r}} = \dot{r}_{ref}$.*

We discuss how to calculate the h_k below in Section III-E.

D. Tracking a time-varying reference velocity

With the preparation of tracking controller analysis in the above subsections, in this subsection we will consider the most general case. We will show the design of a general form of velocity tracking controller to regulate the group centroid velocity that aims to track a desired time-varying reference velocity $\dot{r}_{\text{ref}}(t) = v_{\text{ref}}(t)e^{i\theta_{\text{ref}}(t)}$. The equation of the reference velocity can be written as (see e.g., [21] and [22])

$$\begin{aligned}
\dot{r}_{\text{ref}} &= v_{\text{ref}(t)} e^{i\theta_{\text{ref}}(t)} \\
\dot{\theta}_{\text{ref}} &= \kappa_{\text{ref}}(t) \\
\dot{v}_{\text{ref}} &= a_{\text{ref}}(t)
\end{aligned} \quad (25)$$

where $\kappa_{\text{ref}}(t)$ and $a_{\text{ref}}(t)$ can be time-varying functions. To avoid cumbersome notations we will omit the argument t in the following analysis.

Theorem 3. *Suppose the time-varying reference velocity* (25) *satisfies the conditions in Proposition 1 and the initial headings of all the vehicles are not aligned with the initial phase of the reference velocity. Consider the following steering control law*

$$u_k^{velocity} = -\gamma \left\langle \dot{\hat{r}} - \dot{r}_{ref}, iv_k e^{i\theta_k} \right\rangle + h_k \quad (26)$$

where γ is a positive control gain and the additional control terms h_k that are designed for tracking a time-varying reference velocity satisfy

$$\frac{1}{n}\sum_{k=1}^{n} iv_k e^{i\theta_k} h_k = iv_{ref} e^{i\theta_{ref}} \kappa_{ref} + a_{ref} e^{i\theta_{ref}} \quad (27)$$

for $k = 1, \cdots, n$. Then the equilibrium set at which $\dot{\hat{r}} = \dot{r}_{ref}$ is asymptotically stable and all other equilibria are unstable. The above control law (26) *with the additional input* (27) *will almost globally asymptotically stabilize the group centroid velocity to the desired reference velocity $\dot{r}_{ref}$.*

Theorem 3 is a generalization of both Theorem 2 and Theorem 1 and it treats the most general case for tracking a *time-varying* reference velocity. If the headings of all the vehicles are not all synchronized or anti-synchronized with each other along time, then the control terms h_k are guaranteed to exist. We note here that there exist multiple choices for the additional controller term h_k in the right hand side of (26), which will be discussed in the next subsection.

Proof. The proof takes similar steps as that in Theorem 1. The differences lie in the *feedforward control* term h_k to address the time-varying terms in the reference velocity $\dot{r}_{\text{ref}}$. Again, we denote the velocity tracking error as $\dot{\tilde{r}} := \dot{\hat{r}} - \dot{r}_{\text{ref}}$. Note that

$$\ddot{\hat{r}} = \frac{1}{n}\sum_{k=1}^{n} v_k e^{i\theta_k} i\dot{\theta}_k = \frac{1}{n}\sum_{k=1}^{n} iv_k e^{i\theta_k} u_k^{\text{velocity}} \quad (28)$$

and

$$\ddot{r}_{\text{ref}} = iv_{\text{ref}} e^{i\theta_{\text{ref}}} \kappa_{\text{ref}} + a_{\text{ref}} e^{i\theta_{\text{ref}}} \quad (29)$$

According to (26), the dynamics for the velocity tracking error can be calculated as

$$\ddot{\tilde{r}} = \ddot{\hat{r}} - \ddot{r}_{\text{ref}}$$

$$= -\frac{\gamma}{n} \sum_{k=1}^{n} i v_k e^{i\theta_k} \left\langle \dot{\hat{r}} - \dot{r}_{\text{ref}}, i v_k e^{i\theta_k} \right\rangle \qquad (30)$$

We consider the same Lyapunov function $V = \frac{1}{2} \|\dot{\hat{r}} - \dot{r}_{\text{ref}}\|^2$ which measures the difference between the current centroid velocity and the desired reference velocity. Note that $V(\dot{\tilde{r}}) \geq 0$ and $V(\dot{\tilde{r}})$ is zero if and only if $\dot{\hat{r}} = \dot{r}_{\text{ref}}$, or equivalently $|\dot{\tilde{r}}| = 0$. The derivative of V along the trajectories of the velocity tracking error system (30) can be calculated as

$$\dot{V} = \left\langle \dot{\hat{r}} - \dot{r}_{\text{ref}}, \ddot{\hat{r}} - \ddot{r}_{\text{ref}} \right\rangle$$

$$= \left\langle \dot{\hat{r}} - \dot{r}_{\text{ref}}, -\frac{\gamma}{n} \sum_{k=1}^{n} i v_k e^{i\theta_k} \left\langle \dot{\hat{r}} - \dot{r}_{\text{ref}}, i v_k e^{i\theta_k} \right\rangle \right\rangle$$

$$= -\frac{\gamma}{n} \sum_{k=1}^{n} \left\langle \dot{\hat{r}} - \dot{r}_{\text{ref}}, i v_k e^{i\theta_k} \right\rangle^2 \leq 0 \qquad (31)$$

By LaSalle's Invariance Principle and similar arguments as in the proof of Theorem 1, it can be proven that the desired equilibrium in which $\dot{\tilde{r}} = 0$ in the largest invariant set is asymptotically stable, which indicates the time-varying reference velocity can be successfully tracked. Again, Proposition 1 guarantees the existence of the desired equilibrium at which $|\dot{\tilde{r}}| = 0$. A similar analysis involving the Hessian matrix shows all other equilibrium points with $|\dot{\tilde{r}}| \neq 0$ are unstable. $\qquad \square$

E. Discussion

In this subsection we discuss how to design the control terms h_k in Theorems 2 and 3. The control terms h_k in (20) and (26) serve as feedforward controls which are necessary to track the *time-varying* component of the reference velocity.

By denoting $h = [h_1, h_2, \cdots, h_n]^T$ and separating a complex variable into real part and complex part in the form $e^{i\theta} := [\cos(\theta), \sin(\theta)]^T$, one obtains the left-hand side of (20) and (27) in the following equivalent form:

$$\frac{1}{n} \sum_{k=1}^{n} i v_k e^{i\theta_k} h_k$$

$$= \frac{1}{n} \begin{bmatrix} -v_1\sin(\theta_1) & -v_2\sin(\theta_2) & \cdots & -v_n\sin(\theta_n) \\ v_1\cos(\theta_1) & v_2\cos(\theta_2) & \cdots & v_n\cos(\theta_n) \end{bmatrix} h$$

$$:= Ah \qquad (32)$$

The right-hand sides of (20) and (27) are rewritten respectively as

$$b_1 := i v_{\text{ref}} e^{i\theta_{\text{ref}}} \kappa_{\text{ref}} = \begin{bmatrix} -v_{\text{ref}}\sin(\theta_{\text{ref}})\kappa_{\text{ref}} \\ +v_{\text{ref}}\cos(\theta_{\text{ref}})\kappa_{\text{ref}} \end{bmatrix} \qquad (33)$$

$$b_2 := i v_{\text{ref}} e^{i\theta_{\text{ref}}} \kappa_{\text{ref}} + a_{\text{ref}} e^{i\theta_{\text{ref}}}$$

$$= \begin{bmatrix} a_{\text{ref}}\cos(\theta_{\text{ref}}) - v_{\text{ref}}\sin(\theta_{\text{ref}})\kappa_{\text{ref}} \\ a_{\text{ref}}\sin(\theta_{\text{ref}}) + v_{\text{ref}}\cos(\theta_{\text{ref}})\kappa_{\text{ref}} \end{bmatrix} \qquad (34)$$

Then the calculation of h is equivalent to solving a linear equation with a standard form $Ah = b_1$ or $Ah = b_2$. Since

$A \in \mathbb{R}^{2 \times n}$, a sufficient condition to guarantee the existence of the solution is $\text{rank}(A) = 2$. For the n-vehicle group, the rank condition is satisfied if and only there is if at least one pair of vehicles whose headings are not aligned or anti-aligned (i.e., $\theta_i \neq \theta_j$ or $\theta_i \neq \theta_j + \pi$ for at least one pair of vehicles i, j). In the case of a two-vehicle group, a unique solution exists as $h = A^{-1}b$ when the two vehicles are not aligned or anti-aligned in their headings. For an n-vehicle group, given that the rank condition is satisfied, the solution is not unique and this provides flexibility in the controller design, while a standard least 2-norm solution could be preferred.

Remark 4. *The reference velocity tracking in the tracking control framework is inspired by the previous papers [18], [22]. In contrast, here we are considering a heterogeneous vehicle group with constant non-identical speeds for individual vehicles, which is more general than [18], [22] that discussed tracking control with unit-speed unicycle-type agents. The present results are also extensions of the tracking control strategies for unit-speed unicycles using two special motion primitives (i.e. circular motion and parallel motion) discussed in [18]. A rigorous proof for the convergence of velocity tracking is presented, which is lacking in [22]. Also, the non-identical speed constraints in the group present limitations for a successful tracking; note we have stated explicit necessary conditions on the maximum reference speed and the minimum vehicle speed in Proposition 1 for the tracking controller design.*

IV. CONTROLLER DESIGN PHASE II: REFERENCE TRAJECTORY GENERATION AND SPACING CONTROL

A. Reference velocity generation for target trajectory tracking

In the above section we have designed reference velocity tracking controllers so that the group centroid of the fixed-wing UAVs can successfully track a reference trajectory by matching a reference velocity. In order to guarantee a successful tracking of a target, the reference trajectory should include both the target's trajectory and velocity in the construction of the reference velocity. We propose the following reference velocity

$$\dot{r}_{\text{ref}} = \dot{r}_{\text{target}} + w(r_{\text{target}} - \hat{r}(t)) \qquad (35)$$

where $w > 0$ is a weighting parameter on the relative position between the target r_{target} and the group centroid $\hat{r}(t)$. The weighting parameter w can be used to adjust the convergence speed of position tracking. A larger value of w puts more weights on asymptotically tracking the position of the target, which enables a fast track to the target's trajectory. If initially the group centroid $\hat{r}(t)$ is collocated with the target position, then the target velocity can be used as the reference velocity. Otherwise, the relative position term $(r_{\text{target}} - \hat{r}(t))$ is involved in the reference velocity as a feedback term to guarantee a successful tracking to the target. The following lemma shows that by using the constructed reference velocity in (35) and the velocity tracking controller in Section III, the target's trajectory can be asymptotically tracked.

Lemma 2. *With the reference velocity tracking controller in (26) designed in Section III., and the constructed reference*

velocity in (35)*, the centroid of the fixed-wing UAV group will be asymptotically stabilized to match the target trajectory.*

Proof. As proved in Theorem 3, the designed reference velocity tracking controller (26) guarantees an asymptotic convergence of the group centroid velocity to the reference velocity. Denote $\alpha(t) = \dot{r}_{\text{ref}} - \dot{\hat{r}}(t)$ as the tracking difference between the reference velocity and the centroid velocity. Then one has $\alpha(t) \rightarrow 0$ by virtue of Theorem 3. From (35) we have the following equivalent equation

$$\dot{\hat{r}}(t) - \dot{r}_{\text{target}} = -w(\hat{r}(t) - r_{\text{target}}) - \alpha(t) \qquad (36)$$

Denote $\beta(t) = \hat{r}(t) - r_{\text{target}}$ as the trajectory tracking error between $\hat{r}(t)$ and r_{target}. Then one has $\dot{\beta}(t) = -w\beta(t) - \alpha(t)$. Since $w > 0$ and $\alpha(t) \rightarrow 0$, one obtains $\beta(t) \rightarrow 0$ which indicates that the trajectory tracking error converges to zero asymptotically. □

In practice one can design the weight w as a distance-dependent function (i.e., $w(t) := w(\rho)$ where $\rho = \|r_{\text{ref}}(t) - r_{\text{target}}\|$) to adjust the convergence speed in different phases of the tracking process. Furthermore, since in the limit there holds $\dot{r}_{\text{ref}} \rightarrow \dot{r}_{\text{target}}$, in order to ensure the condition in Proposition 1 is satisfied, we should also impose the condition on the target velocity $v_{\min} \geq \|v_{\text{target}}(t)\|$ to ensure a feasible tracking.

B. Vehicle-target spacing control

In this subsection we design the spacing controller u^{spacing} to ensure all vehicles stay with a bounded distance to the group centroid. As noted above, there exists a trade-off between the design of the velocity tracking controller and a spacing control. We will follow a similar idea as in [34], [35] for the spacing controller design. We first present the following condition for an admissible spacing control that does not affect the performance of the centroid velocity tracking control.

Lemma 3. *Denote the spacing control vector* $u^{spacing} = [u_1^{spacing}, u_2^{spacing}, \cdots, u_n^{spacing}]^T$ *and define the matrix A as in* (32)*. The additional spacing control $u^{spacing}$ satisfying*

$$u^{spacing} \in ker(A) \qquad (37)$$

preserves the asymptotic tracking performance of the reference velocity by the group centroid (i.e., $\hat{r} \rightarrow \dot{r}_{ref}$ as $t \rightarrow \infty$).

Proof. We consider the same Lyapunov function as used in Section III. The controller u^{velocity} designed in (26) is used here as an example for the velocity tracking analysis. The time derivative of the Lyapunov function along the solution of the system (6) with the combined controller (7) can be calculated

as

$$\dot{V} = \left\langle \dot{\hat{r}} - \dot{r}_{\text{ref}}, \ddot{\hat{r}} - \ddot{r}_{\text{ref}} \right\rangle$$

$$= \left\langle \dot{\hat{r}} - \dot{r}_{\text{ref}}, \frac{1}{n} \sum_{k=1}^{n} iv_k e^{i\theta_k} u_k^{\text{velocity}} - \ddot{r}_{\text{ref}} \right\rangle$$

$$+ \left\langle \dot{\hat{r}} - \dot{r}_{\text{ref}}, \underbrace{\frac{1}{n} \sum_{k=1}^{n} iv_k e^{i\theta_k} u_k^{\text{spacing}}}_{=0} \right\rangle$$

$$= \left\langle \dot{\hat{r}} - \dot{r}_{\text{ref}}, \frac{1}{n} \sum_{k=1}^{n} iv_k e^{i\theta_k} u_k^{\text{velocity}} - \ddot{r}_{\text{ref}} \right\rangle \leq 0 \qquad (38)$$

Note that the equality in the third line of the above (38) is due to the condition in (37). Therefore, $\dot{V}$ is invariant for any control u^{velocity} of (37), and is negative semidefinite according to the controller property. The remaining analysis is similar to the proof of previous theorems in Section III and is omitted here. □

For a vehicle group with $n > 2$ vehicles with non-aligned headings, the matrix A is of full row rank and so has a null space of dimension $n - 2$, which leaves motion freedoms for designing the spacing controller. However, it is challenging to design an admissible control input that lies in $\ker(A)$ while also keeping all vehicles within a reasonable spacing around the centroid. In particular, an analytical solution for an admissible spacing control u^{spacing} is not available, while a numerical solution is usually expensive. Actually, even for the coordination control of *identical unit-speed* vehicles, it is still an open problem to design explicit controllers to satisfy the above constraint and design requirement (see more in-depth discussions in [35, Chapter 2]).

Inspired by [36] and [37], we consider an alternative approach based on the *beacon control law* proposed by Paley et al. [37], [38] to design an intuitive spacing control. The idea is to allow each vehicle to perform limited circular trajectories around a chosen beacon point in the reference trajectory path. In this way, the spacing control takes a position feedback from a reference trajectory, and is designed as

$$u_k^{\text{spacing}} = -(\omega_0 + \gamma\omega_0 \left\langle r_k - r_{\text{ref}}, v_k e^{i\theta_k} \right\rangle \qquad (39)$$

where ω_o is a positive parameter for adjusting the period in the circular motion. It has been proved in [27], [37], [38] that the above control (in the absence of velocity tracking control) guarantees constant-speed vehicles performing circular motions around a reference point r_{ref}. It has also been shown in [36] by using simulation examples that the above spacing control will ensure that all the vehicles move and remain close to the centroid. We note that this control is generally not an admissible one in the null space of A satisfying the condition in Lemma 3 and therefore a perfect velocity tracking performance is not guaranteed by the addition of the spacing controller. However, as demonstrated by numerous numerical simulations and experiments in the next sections, such a spacing control law can ensure all agents stay close to the group centroid while the group centroid position tracks the target trajectory.

An alternative solution with a small number of UAVs is to consider projecting (39) onto the non-zero kernel of A. The philosophy of designing u^{spacing} without affecting the centroid velocity tracking task is inspired by [22], [39], and is actually in the broad framework of null-space-based (NSB) robotic behavior control proposed in [39]–[41]. In the framework of NSB approach, each sub-task is assigned a certain priority and the control term for a sub-task with a lower priority should live in the null space of the control task space of those with higher priorities. However, the NSB approach is often computationally expensive and unscalable, which may not be suitable for real-time tracking control and may quickly become infeasible when the number of UAVs increases. We also remark that in the two-step controller design we do not assign any priority in each sub-task. Since an analytical and perfect solution for both subtasks in the target tracking control is hard to find as shown in [35], one may consider ad-hoc solutions (see e.g. [24]) by taking into account different way points in the target trajectory to be used as feedback information and designing a *switching* tracking controller to ensure tracking convergence and boundedness. However, in this way analytical convergence results are hard to obtain.

V. SIMULATION EXAMPLES

We refer the readers to [29] for several typical simulation examples that demonstrate the effectiveness and performance of the proposed tracking controllers for a group of fixed-wing UAVs with constant but non-identical airspeeds. Two sets of numerical simulation examples were given in [29], one for collective tracking of a target with constant velocity, and the other for collective tracking of a target with time-varying (but bounded) velocity. In both cases, the proposed tracking controllers guarantee a desirable tracking performance through vehicle centroid and bounded tracking distance errors for a group of constant-speed vehicles to collaboratively track moving targets.

VI. EXPERIMENTAL VERIFICATION

The purpose of this section is to validate the proposed algorithms with fixed-wing aircraft in a series of experiments. This validation is not a mere extension of the theoretical work. In particular, we have reconsidered some assumptions in the theoretical analysis that are no longer satisfied in a real distributed control system. For example, several issues exist in practice such as the presence of delays in the transmission of information, the non-synchronization of clocks, or sensors on different vehicles that are biased with respect each other. Some of these issues may potentially have a significant impact on the performance of the overall system, especially in a decentralized control setting [42], [43]. Therefore, one of the goals of this section is to validate the performance of the proposed algorithms in practice even when some important factors have been omitted in the development of theoretical analysis.

The experimental setup consists of one Parrot Bebop2 rotorcraft (serving as a target to be tracked) and three fixed-wing aircraft labeled as Wing 2, 3 and 4, respectively. All

Fig. 4: The three fixed-wing UAVs employed in the experiments. They have a 120cm wingspan and weight around 800grams. The vehicles are powered by the open-source autopilot *Paparazzi*.

the vehicles are equipped with the open-source autopilot *Paparazzi*[4], which allows a rapid prototyping for distributed aerial systems as shown in our recent works [27], [28]. This platform also enables third parties to quickly implement and use for other purposes our proposed algorithms[5].

We choose the scenario of target trajectory tracking described in Section IV.A since it covers most of the presented results in this paper. In particular, we assign a rotor-craft as an independent target which flies at the ground speed of 2 m/s. The three aircraft fly at constant speeds between 10 m/s and 16 m/s while they execute onboard their control actions (26) with $\dot{r}_{\text{ref}}$ given by (35) and a positive distance-dependent weight $w(\rho) = \frac{1}{\rho}(1 - e^{-0.1\rho})$ (we remind that $\rho = \|r_{\text{ref}}(t) - r_{\text{target}}(t)\|$), and the spacing controller (39) with $\omega_0 = 0.25$ rads/sec. The chosen gains for (26) and (35) were 0.001 for both cases. The relative positions between the vehicles are calculated onboard by having the UAVs broadcasting their absolute positions obtained by a GPS. We employ *X-Bee* modules which create a network among them. This network supports air-to-air communication without ground intervention. This feature is already implemented and available in the *Paparazzi* project. The broadcasting frequency for the target is 5Hz, whereas for the aircraft is 10Hz. Indeed, the fact that there exist communication losses (i.e., communication dropouts over short intervals) between aircraft, and that the aircraft process the information at different times, leads to possible discrepancies among the three vehicles about the relative positions.

The experiment was performed in a radio control club in Muret, a city close to Toulouse in France. The wind velocity had an average speed of 3 m/s and an almost constant direction. Note that this wind speed has a noticeable impact on the ground speed of the aircraft. Nevertheless, as the experimental results indicate, such a wind speed does not have an impact on the intended performance of the algorithm. We consider

---

[4]For more information, see http://wiki.paparazziuav.org.

[5]See the master branch at https://github.com/paparazzi/paparazzi, or the experimental branch *collective_tracking_control* at https://github.com/noether/paparazzi.
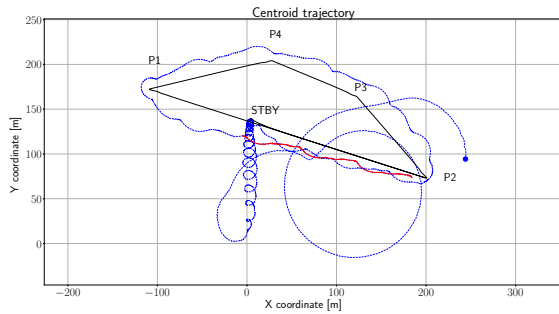
Fig. 5: The trajectory of the centroid of the team in blue color (the dot represents the starting point at time $t = 90$ secs. The red color represents the centroid's trajectory for the last two minutes of the mission. The black color denotes the trajectory of the target. During the first part of the mission, the target is on the ground at STBY. During the second part, the target flies at 2m/s following the closed path between all the waypoints.
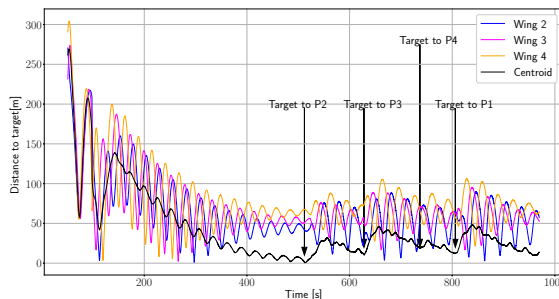

Fig. 6: The mission starts at time $t = 90$secs. The centroid of the team converges to the STBY point asymptotically, reaching almost zero at time $t = 510$ secs. Then the target starts flying visiting the rest of the waypoints. Every time the target changes abruptly its velocity, the algorithm needs time to cause the centroid to converge again to be close to the target's position.

θ as the heading angle (vector velocity), and not the attitude *yaw* angle. If there is no wind, both angles are the same in our setup. In practice, when we consider the heading instead of the yaw for the unicycle model, the aircraft ends up compensating the lateral wind by *crabbing* so that aerodynamic angle *sideslip* is almost zero[6].

We divide the mission into two stages. Firstly, we place the rotorcraft on the ground at the waypoint STBY. Then we launch the three aircraft to orbit around the waypoint C. We denote in green color the starting circular trajectory in Figure 7a. At time $t = 90$ secs, the three aircraft start the algorithm. With our setup and initial conditions, it takes around seven minutes until the centroid of the team converges to STBY

---

[6]Crabbing happens when the inertial velocity makes an angle with the nose heading due to wind. *Slipping* happens when the aerodynamic velocity vector makes an angle (sideslip) with the body ZX plane. Slipping is (almost) always undesirable, because it degrades aerodynamic performance. Crabbing is not an issue for the aircraft.

(see Figures 6 and 7b). Secondly, after the first convergence, the target starts flying following a closed path with a speed of 2m/s. The target changes its velocity every time it travels to a different waypoint. Then, the algorithm successfully drives the centroid of the team to converge again to the target's moving position as illustrated in Figure 6.

VII. CONCLUSIONS

Fixed-wing UAVs have found increasing applications in both civilian and defense fields in recent years. Compared with rotary-wing UAVs, fixed-wing UAVs in general feature significantly larger flight ranges and longer flight duration which are more suitable for autonomous tasks such as surveillance, circumnavigation and tracking. However, a key challenge in fixed-wing UAV coordination and control is the airspeed constraint associated with maintaining stable flight. In this paper, we investigate the possibility and applicability of using multiple fixed-wing UAVs with constant and possibly non-identical speeds to conduct a collaborative tracking task of a moving target. Inspired by previous papers (e.g. [21], [22]), a systematic framework is proposed for the collaborative target-tracking control. We have used the group centroid as a representative of the overall UAV group in the tracking process. The design of the tracking controller consists of two parts: the reference velocity tracking control that regulates the group centroid to track a reference velocity, and a spacing controller that ensures all vehicles keep close to the group centroid. The reference velocity involves the target velocity as well as the relative position to the target as feedback to ensure the group centroid tracks the target trajectory. We have also discussed the trade-offs and limitations of using fixed-wing UAVs to track a moving target, and conditions that ensure a feasible tracking. Despite the strict constraint of differing constant speeds, we have provided a positive solution showing that fixed-wing UAVs are applicable for performing autonomous target tracking tasks as a group, which is supported by both numerical simulations and real-life experiments involving a group of three fixed-wing UAVs, subject to limited wind disturbance. In the future research, we will further investigate the effect of wind flows on fixed-wing UAV coordination in general collaborative control tasks.

REFERENCES

[1] J. G. Manathara, P. Sujit, and R. W. Beard, "Multiple UAV coalitions for a search and prosecute mission," *Journal of Intelligent & Robotic Systems*, vol. 62, no. 1, pp. 125–158, 2011.

[2] B. D. O. Anderson, B. Fidan, C. Yu, and D. Walle, "UAV formation control: theory and application," in *Recent advances in learning and control*, pp. 15–33, Springer, 2008.

[3] R. W. Beard and T. W. McLain, *Small Unmanned Aircraft: Theory and Practice*. Princeton University Press, 2012.

[4] Y. Kang and J. K. Hedrick, "Linear tracking for a fixed-wing UAV using nonlinear model predictive control," *IEEE Transactions on Control Systems Technology*, vol. 17, no. 5, pp. 1202–1210, 2009.

[5] S. A. Quintero, F. Papi, D. J. Klein, L. Chisci, and J. P. Hespanha, "Optimal UAV coordination for target tracking using dynamic programming," in *Proc. of the 2010 49th IEEE Conference on Decision and Control (CDC)*, pp. 4541–4546, IEEE, 2010.

[6] N. Regina and M. Zanzi, "UAV guidance law for ground-based target trajectory tracking and loitering," in *Proc. of the 2011 IEEE Aerospace Conference*, pp. 1–9, IEEE, 2011.

(a) t = 90secs   (b) t = 420secs   (c) t = 685secs   (d) t = 809secs
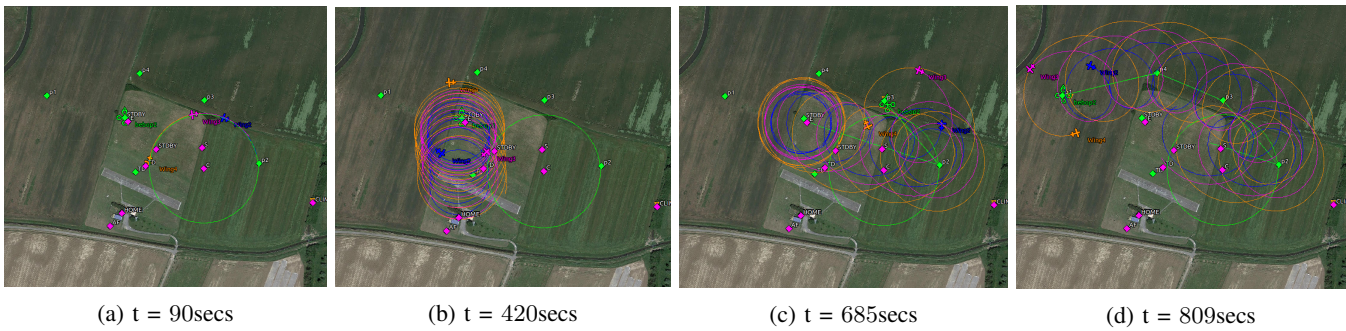
Fig. 7: Screenshots from the *Paparazzi* ground control station during the mission. The screenshot (a) denotes the initial conditions for the aircraft and the target (check Figure 5 for the distances in meters between the waypoints). The screenshot (b) shows the centroid of the team instants before its eventual convergence to the static target at STBY. The screenshots (c) and (d) show the team of fixed-wing UAVs tracking the moving target with their centroid. The rest of the markers on the screenshots that are not commented are waypoints to assist the operators while the aircraft are not executing the algorithm, i.e., on the taking off, standing-by, and landing.

[7] W. Ren and R. W. Beard, "Trajectory tracking for unmanned air vehicles with velocity and heading rate constraints," *IEEE Transactions on Control Systems Technology*, vol. 12, no. 5, pp. 706–716, 2004.

[8] N. Regina and M. Zanzi, "Surface target-tracking guidance by self-organizing formation flight of fixed-wing UAV," in *Proc. of the 2013 IEEE Aerospace Conference*, pp. 1–10, IEEE, 2013.

[9] Z. Lin, B. Francis, and M. Maggiore, "Necessary and sufficient graphical conditions for formation control of unicycles," *IEEE Transactions on Automatic Control*, vol. 50, no. 1, pp. 121–127, 2005.

[10] J. A. Marshall, M. E. Broucke, and B. A. Francis, "Pursuit formations of unicycles," *Automatica*, vol. 42, no. 1, pp. 3–12, 2006.

[11] D. V. Dimarogonas and K. J. Kyriakopoulos, "On the rendezvous problem for multiple nonholonomic agents," *IEEE Transactions on Automatic Control*, vol. 52, no. 5, pp. 916–922, 2007.

[12] S. Mastellone, D. M. Stipanović, C. R. Graunke, K. A. Intlekofer, and M. W. Spong, "Formation control and collision avoidance for multi-agent non-holonomic systems: Theory and experiments," *The International Journal of Robotics Research*, vol. 27, no. 1, pp. 107–126, 2008.

[13] N. Regina and M. Zanzi, "A novel solution for overflight and surveying of a collaborative target with fixed wing UAV," in *Prof. of the AIAA Guidance, Navigation, and Control Conference*, p. 4605, 2012.

[14] T. Liu and Z.-P. Jiang, "Distributed formation control of nonholonomic mobile robots without global position measurements," *Automatica*, vol. 49, no. 2, pp. 592–600, 2013.

[15] B. Fidan, V. Gazi, S. Zhai, N. Cen, and E. Karatas, "Single-view distance-estimation-based formation control of robotic swarms," *IEEE Transactions on Industrial Electronics*, vol. 60, no. 12, pp. 5781–5791, 2013.

[16] L. Briñón-Arranz, A. Seuret, and C. Canudas-de Wit, "Cooperative control design for time-varying formations of multi-agent systems," *IEEE Transactions on Automatic Control*, vol. 59, no. 8, pp. 2283–2288, 2014.

[17] L. Briñón-Arranz, *Cooperative control design for a fleet of AUVs under communication constraints*. PhD thesis, Université de Grenoble, 2011.

[18] R. Sepulchre, D. A. Paley, and N. E. Leonard, "Stabilization of planar collective motion: All-to-all communication," *IEEE Transactions on Automatic Control*, vol. 52, no. 5, pp. 811–824, 2007.

[19] L. Briñón-Arranz, A. Seuret, and A. Pascoal, "Target tracking via a circular formation of unicycles," *Proc. of the 20th IFAC World Congress*, vol. 50, no. 1, pp. 5782–5787, 2017.

[20] N. Moshtagh and A. Jadbabaie, "Distributed geodesic control laws for flocking of nonholonomic agents," *IEEE Transactions on Automatic Control*, vol. 52, no. 4, pp. 681–686, 2007.

[21] R. Sepulchre, D. A. Paley, and N. E. Leonard, "Stabilization of planar collective motion with limited communication," *IEEE Transactions on Automatic Control*, vol. 53, no. 3, pp. 706–719, 2008.

[22] D. J. Klein and K. A. Morgansen, "Controlled collective motion for trajectory tracking," in *Proc. of the American Control Conference*, pp. 5269–5275, IEEE, 2006.

[23] E. W. Justh and P. S. Krishnaprasad, "Equilibria and steering laws for

[24] D. van der Walle, B. Fidan, A. Sutton, C. Yu, and B. D. O. Anderson, "Non-hierarchical UAV formation control for surveillance tasks," in *Proc. of American Control Conference*, pp. 777–782, IEEE, 2008.

[25] N. Moshtagh, N. Michael, A. Jadbabaie, and K. Daniilidis, "Vision-based, distributed control laws for motion coordination of nonholonomic robots," *IEEE Transactions on Robotics*, vol. 25, no. 4, pp. 851–860, 2009.

[26] G. S. Seyboth, J. Wu, J. Qin, C. Yu, and F. Allgower, "Collective circular motion of unicycle type vehicles with nonidentical constant velocities," *IEEE Transactions on Control of Network Systems*, vol. 1, no. 2, pp. 167–176, 2014.

[27] Z. Sun, H. G. de Marina, G. S. Seyboth, B. D. O. Anderson, and C. Yu, "Circular formation control of multiple unicycle-type agents with nonidentical constant speeds," *IEEE Transactions on Control Systems Technology*, vol. 27, no. 1, pp. 192–205, 2019.

[28] H. G. de Marina, Z. Sun, M. Bronz, and G. Hattenberger, "Circular formation control of fixed-wing UAVs with constant speeds," in *Proc. of the 2017 IEEE/RSJ International Conference on Intelligent Robots and Systems*, pp. 5298–5303, IEEE, 2017.

[29] Z. Sun, G. S. Seyboth, and B. D. O. Anderson, "Collective control of multiple unicycle agents with non-identical constant speeds: Tracking control and performance limitation," in *Proc. of the 2015 IEEE Conference on Control Applications (CCA)*, pp. 1361–1366, IEEE, 2015.

[30] E. Xargay, V. Dobrokhodov, I. Kaminer, A. M. Pascoal, N. Hovakimyan, and C. Cao, "Time-critical cooperative control of multiple autonomous vehicles," *Control Systems Magazine, IEEE*, vol. 32, no. 5, p. 49, 2012.

[31] F. Dörfler and F. Bullo, "Synchronization in complex networks of phase oscillators: A survey," *Automatica*, vol. 50, no. 6, pp. 1539–1564, 2014.

[32] P.-A. Absil and K. Kurdyka, "On the stable equilibrium points of gradient systems," *Systems & Control Letters*, vol. 55, no. 7, pp. 573–577, 2006.

[33] Y. Kuramoto, *Chemical Oscillations, Waves, and Turbulence*. Dover Publications, 2003.

[34] D. Kingston and R. Beard, "UAV splay state configuration for moving targets in wind," in *Advances in Cooperative Control and Optimization*, pp. 109–128, Springer, 2007.

[35] D. J. Klein, *Coordinated control and estimation for multi-agent systems: Theory and practice*. PhD thesis, University of Washington, 2008.

[36] A. Pongpunwattana, B. Triplett, and K. Morgansen, "Target tracking control with limited communication and steering dynamics," in *Proc. of IEEE/RSJ International Conference on Intelligent Robots and Systems (IROS)*, pp. 3094–3100, Oct 2007.

[37] D. A. Paley, N. E. Leonard, and R. Sepulchre, "Collective motion: Bistability and trajectory tracking," in *Proc. of the 43rd IEEE Conference on Decision and Control*, vol. 2, pp. 1932–1937, IEEE, 2004.

[38] D. A. Paley, N. E. Leonard, R. Sepulchre, D. Grunbaum, and J. K. Parrish, "Oscillator models and collective motion," *Control Systems Magazine, IEEE*, vol. 27, no. 4, pp. 89–105, 2007.

[39] G. Antonelli, F. Arrichiello, and S. Chiaverini, "Experiments of formation control with multirobot systems using the null-space-based

planar formations," *Systems & Control Letters*, vol. 52, no. 1, pp. 25–38, 2004.

behavioral control," *IEEE Transactions on Control Systems Technology*, vol. 17, no. 5, pp. 1173–1182, 2009.

[40] F. Arrichiello, S. Chiaverini, G. Indiveri, and P. Pedone, "The null-space-based behavioral control for mobile robots with velocity actuator saturations," *The International Journal of Robotics Research*, vol. 29, no. 10, pp. 1317–1337, 2010.

[41] H. Sadeghian, L. Villani, M. Keshmiri, and B. Siciliano, "Task-space control of robot manipulators with null-space compliance," *IEEE Transactions on Robotics*, vol. 30, no. 2, pp. 493–506, 2014.

[42] S. Mou, M.-A. Belabbas, A. S. Morse, Z. Sun, and B. D. O. Anderson, "Undirected rigid formations are problematic," *IEEE Transactions on Automatic Control*, vol. 61, no. 10, pp. 2821–2836, 2016.

[43] H. G. de Marina, M. Cao, and B. Jayawardhana, "Controlling rigid formations of mobile agents under inconsistent measurements," *IEEE Transactions on Robotics*, vol. 31, no. 1, pp. 31–39, 2015.